Review of Palaeobotany and Palynology 268 (2019) 95–108

Contents lists available at ScienceDirect

Review of Palaeobotany and Palynology

journal homepage: www.elsevier.com/locate/revpalbo

Cuticle ultrastructure of *Baiera furcata* from Northeast China and its implication in taxonomy and paleoenvironment

Gaëtan Guignard [a,b], Xiao-Ju Yang [c,*], Yong-Dong Wang [c]

[a] Université Lyon 1, F-69622 Lyon, France
[b] CNRS, UMR 5023 LEHNA, 7-9 rue raphaël Dubois, 69622 Villeurbanne cedex, France
[c] Nanjing Institute of Geology and Palaeontology, Chinese Academy of Sciences, 39 East Beijing Road, Nanjing 210008, China

ARTICLE INFO

Article history:
Received 15 January 2019
Received in revised form 11 May 2019
Accepted 14 May 2019

Keywords:
Baiera
Sphenobaiera
Cuticle ultrastructures
Stomata
Cretaceous

ABSTRACT

A study on the leaf cuticle ultrastructures of *Baiera furcata* from the Lower Cretaceous Huolinhe Formation in East Inner Mongolia, Northeast China, was conducted with transmission electron microscopy (TEM) and elements analysis by Energy Dispersive Spectroscopy (EDS). TEM observation revealed the ultrastructural details from ordinary epidermal cells for both upper and lower cuticles, and stomatal apparatus, which were all made with A2 (granular) and B1 (fibrilous) layers. Additionally, well-preserved cell remnants were also observed. Comparisons with other cuticles of the Ginkgoales were made using statistical measurements and evaluations of some potential Order characteristics, and genus–species characteristics were also emphasized. Two potential ultrastructural groups can be recognized: *Baiera–Sphenobaiera* and *Ginkgo–Ginkgoites–Pseudotorellia*. This is reinforced by EDS element analysis, whereby ratios could also be compared with another closely related Ginkgoalean taxon *Sphenobaiera huangii*. The paleoenvironment significances is discussed, and it seems to support the TEM and EDS results. It indicates a signature in the cuticle fine details of *Sphenobaiera*, which has experienced a putatively warmer paleoenvironment than that of *Baiera*.

1. Introduction

The application of transmission electron microscopy (TEM) in paleobotany beginning in the late 1980s (e.g., Archangelsky and Taylor, 1986; Archangelsky et al., 1986) has considerably contributed to our knowledge of the cuticle ultrastructure of fossil plants. Until now, many groups, such as pteridosperms (Guignard et al., 2001, 2004; Thévenard et al., 2005), Cycadeoidales (Villar de Seoane, 2005), Bennettitales (Villar de Seoane, 1999, 2001, 2003), Czekanowskiales (Zhou and Guignard, 1998), Ginkgoales (Guignard and Zhou, 2005; Wang et al., 2005; Del Fueyo et al., 2013) and conifers (Archangelsky and Del Fueyo, 1989; Barale et al., 1992; Nosova et al., 2016) have been studied for their cuticle ultrastructure by using the TEM technique. Among them, special interest has been given to the cuticle ultrastructure in the family Cheirolepidiaceae in the last 30 years, and nearly 10 species belonging to 6 genera have been studied by TEM (Archangelsky and Taylor, 1986; Guignard et al., 1998; Villar De Seoane, 1998; Zhou et al., 2000; Yang et al., 2009; Mairot et al., 2014; Guignard et al., 2017; Yang et al., 2018). However, few studies have been conducted on the cuticle ultrastructure of Ginkgoales. At present, only the leaf cuticles ultrastructures of living *Ginkgo biloba* L. and fossil *Ginkgo yimaensis* Zhou et Zhang from the Middle Jurassic of China (Guignard and Zhou, 2005), *Ginkgoites skottsbergii* Lundblad (Guignard et al., 2016) and *Ginkgoites ticoensis* Archang. (Del Fueyo et al., 2013) from the Early Cretaceous of Argentina, and *Sphenobaiera huangii* (Sze) Hsü from the Middle Jurassic of China (Wang et al., 2005) have been described.

*Baiera*Braun (1843) is one of the oldest fossil foliage types of Ginkgoales. It is among the most common genera of ginkgoalean vegetative leaves in the Mesozoic of both Laurasia and Gondwana. Hundreds of species of *Baiera* have been reported since the establishment of the genus, and in China, approximately 31 species have been documented from Permian to Neogene (Zhou and Wu, 2006). Affiliated reproductive structures were poorly known until Zhou and Zhang (1992) described ovulate organs of *Yimaia* as being intimately associated with *Baiera hallei* Sze in the Middle Jurassic of Henan, China. Similar ovulate organs ascribed to *B. muensteriana* (Sternberg) (Braun, 1843) were restudied by Kirchner (1992) based on the original material from the Liassic of Franconia, Germany. The progress made on reproductive structures has contributed to our knowledge of the classification and relationships of *Baiera* (Kirchner, 1992; Zhou and Zhang, 1992). In China, ovulate organs of *Yimaia* were also found to be associated with *Baiera*-type leaves from the Middle Jurassic of Qinghai Province, Northwest China, and the associated leaf segments of *Baiera* bear a resemblance to that of the Yorkshire Middle Jurassic species *Baiera furcata* (Lindley et Hutton)

* Corresponding author.
E-mail address: xjyang@nigpas.ac.cn (X.-J. Yang).

https://doi.org/10.1016/j.revpalbo.2019.05.006
0034-6667/

Braun (Wu et al., 2006). This species is the most widespread leaf around the world (Harris et al., 1974; Zhou and Wu, 2006). In China, this species have been recorded from more than thirty localities based on impression specimens from the Upper Triassic to the Early Cretaceous (Zhou et al., 2019).

In this paper, the foliage of *Baiera furcata* was reinvestigated with an emphasis on the cuticular ultrastructure by using TEM and element analysis EDS (Energy Dispersive Spectroscopy) to study the cuticles and the rock matrix, respectively, of the plant-bearing beds. To compare with *Sphenobaiera huangii* formerly studied in TEM (Wang et al., 2005), an EDS element analysis of this taxon has been added to this paper. The paleoenvironment feature is also discussed based on the ultrastructure of the cuticle and element analyses of the rock matrix, incorporating evidence from the associated fossil plants (Deng, 1995).

2. Material and methods

The specimens studied in the present paper were collected from a thin gray mudstone at the lower coal-bearing bed of the Early Cretaceous Huolinhe Formation in the Huolinhe coal mine (45°29′06″ N, 119°34′30″ E.) of Holingola City of the Inner Mongol Autonomous Region, northeastern China (Fig. 1). The gray mudstone contains abundant plants of compressed ginkgoalean leaves, and most of them are dominated by *Baiera furcata* and its fragments (Fig. 2). The cuticle structure of *Baiera furcata* from the Early Cretaceous Huolinhe Formation in Holingola has been described (Deng, 1995), here an emphasis was put on the cuticular ultrastructure reinvestigated by using TEM.

Pieces of cuticle were treated with hydrofluoric acid (HF 70%) for 12–18 h and were subsequently macerated in Schulze's solution (concentrate nitric acid and potassium chlorate) for approximately 12 h. When they became yellow and translucent, they were rinsed with water, then treated with dilute ammonium hydroxide (5%) for a few seconds to half a minute, and then thoroughly rinsed with water. The samples for TEM were prepared following Lugardon (1971), which was used for living plant cuticles (conifers and angiosperms; Bartiromo et al., 2012, 2013). In total, 11 pieces of the cuticle samples from 6 leafy segments were embedded in Epon resin: 5 blocks were made from 10 treated materials, and 1 block was made from 1 untreated material for comparison (not illustrated in plates, as the sections were of unfavorable quality). From these, 110 ultrathin sections of 60–70 nm thickness were made and were collected on uncoated 300 mesh copper grids (100 transversal sections, i.e., perpendicular to the leaf length; 10 longitudinal sections, i.e., parallel to the leaf length). Some attempts were also made with 10 single-slot oval whole 2 mm/1 mm uncoated copper grids. Ultrathin sections were selected, observed and photographed with a Philips CM 120 TEM at 80 kV, at the Centre de Technologie des Microstructures (CTμ) of Lyon-1 University, France.

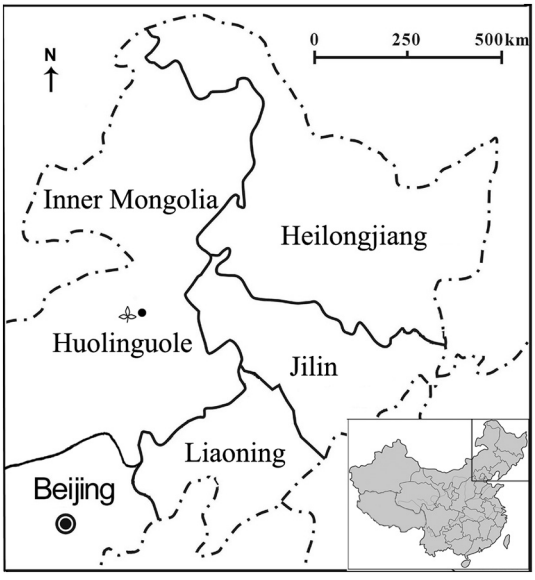

Fig. 1. Sketched geographic map showing the fossil locality (45°29′06″ N, 119°34′30″ E.) Holingola in East Inner Mongolia, Northeast China.

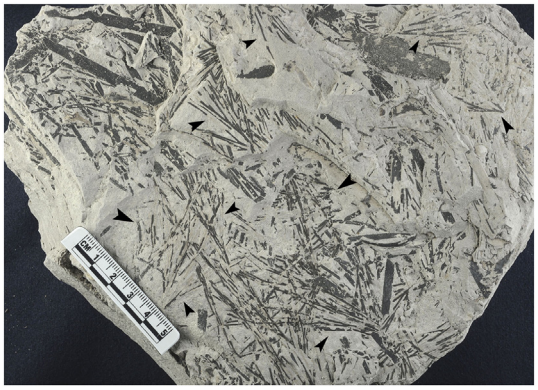

Fig. 2. *Baiera furcata* (arrows) from the Early Cretaceous Huolinhe Formation, Holingola, Inner Mongolia, China (Specimen PB 22980).

EDS (energy dispersive spectroscopic) analysis was performed on the TEM using SIRIUS SD ENSOTECH and IDFIX software with acceleration voltage 120 kV, spot sizes 1–3, processing time 60–120 s, constant time of 4 μs. Fifteen copper 300 mesh uncoated grids of the present material were made, devoid of uranyl acetate and lead citrate staining. To compare with *Sphenobaiera huangii*, five sections mounted on grids were prepared for this taxon, which had already been studied by TEM (Wang et al., 2005). Among the available elements, Cu and Al were eliminated in the results as belonging to the grid, Os as part of the embedding technique, Si as part of the oils used in the TEM, and C and O also as major parts of the EPON embedding resin. Measurements were evaluated with a Mann–Whitney test, using XLSTAT version 2018.2 software, which provided diagrams of the results that were included in this paper. For TEM and EDS statistics, XLSTAT 2019.1 was used (Addinsoft, 2019, XLSTAT statistical and data analysis solution. Long Island, NY, USA. https://www.xlstat.com.). Element analyses of the matrix containing fossil plants from the two localities were undertaken using an energy dispersive X-ray (EDX) system attached to LEO-1530VP in Nanjing.

The hand specimens of *Baiera furcata* (number PB22980) and *Sphenobaiera huangii* (number PB20041) is housed in the Nanjing Institute of Geology and Palaeontology, Chinese Academy of Sciences, China. TEM material and negatives are stored in the Lyon-1 University, Villeurbanne, France.

3. Results

3.1. Cuticle ultrastructure

The cuticle ultrastructure of the ordinary epidermal cells (Plates I–II), and the subsidiary and guard cells of the stomatal apparatus were observed in detail (Plate III). All statistical data (Table 1; Supplementary material A) were calculated using 30 measurements. Four types of cuticles, two for ordinary epidermal cells and two for stomatal apparatus cells, were discerned. All cuticular membranes (CM) consisted of A2 granular layer (belonging to the cuticle proper [CP]) and B1 fibrilous and somewhat reticulate layer(belonging to the cuticular layer [CL]). The data described below are the mean values, and the percentage of each component of the cuticle is also shown (Table 1; Supplementary material A).

Two types of cuticles were observed for the ordinary epidermal cell cuticle (Plates I, II): the upper cuticle was thicker, about 2.63 μm in mean thickness (Table 1), with more of the A2 layer than the B1 layer

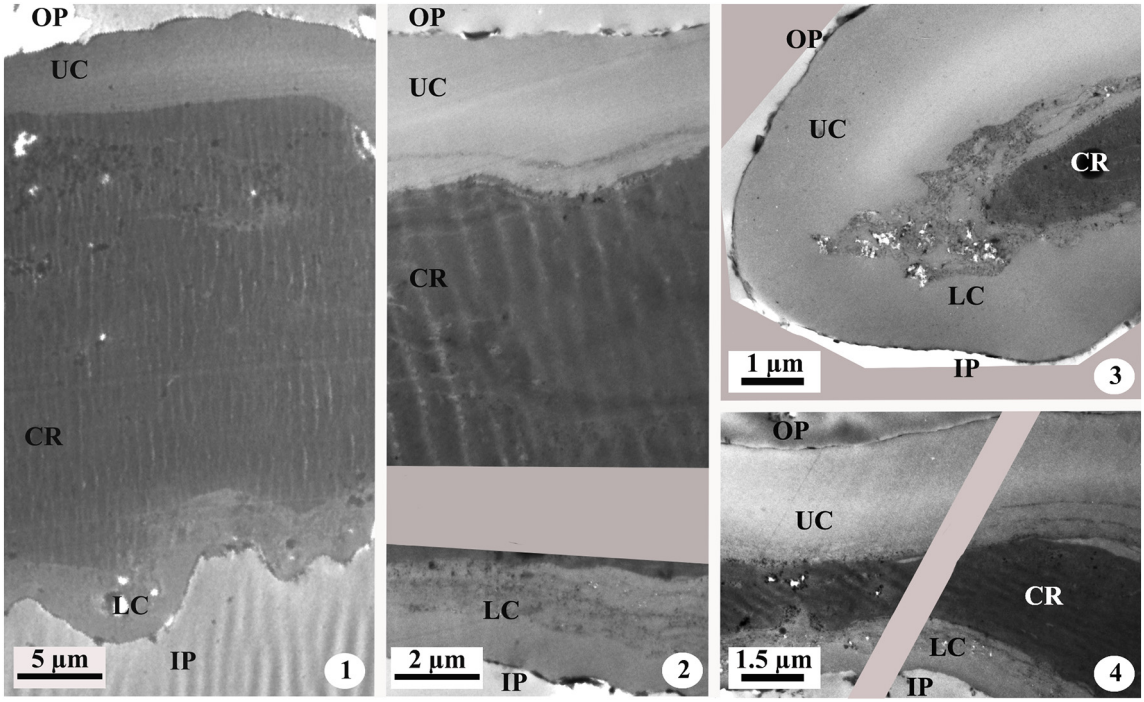

Plate I. Ultrastructural transmission electron micrographs, ordinary epidermal cell cuticles of *Baiera furcata* (specimen PB22980), general views. OP = outer part, IP = inner part, UC = upper cuticle, LC = lower cuticle, CR = cell remnants. All micrographs are from untreated material, transversal sections. 1, 2, 4. Sections of leaves, showing the thicker upper cuticle and thinner lower cuticle, separated by cell remnants where details of cell are hardly distinguishable. 3. One edge of section of leaf, with the two thicker upper and thinner lower cuticles connected and their different thicknesses. Cell remnants are visible in the middle part of the leaf.

in based on the mean (72.24% versus 27.76%, respectively); the lower cuticle was thinner (1.53 µm in mean), with less thickness of the A2 layer than the B1 layer (43.79% versus 56.21%). This is true for all parts of the leaf sections, including the edges, where the two cuticles are linked but showing different thicknesses (Plate I, 3). In the details of the ultrastructure, for both upper (Plate II, 1–10) and lower (Plate II, 11–15) cuticles, the fibrils of the B1 layer make various schemes of reticulum that mixed with other straight fibrils. They usually oriented parallel to the inner surface of the cuticle (Plate II, 6–8, 14–15) with quite few of them oriented perpendicularly (Plate II, 10). Amorphous and darkly stained cell remnants are present. The bottom of the B1 layer is directly connected with cell wall remnants, which are visible in many cases (Plate II, 8, 13, 15). The lower cuticle shows many foldings (Plate II, 13), and the cell remnants are apparently absent from these foldings.

Although this taxon is amphistomatic, the number of stomatal apparatuses is too rare on the upper cuticle sections, and only those from lower cuticles were observed in details. The A2 and B1 layers were also observed in the subsidiary and guard cell cuticles (Plate III). In cases where the whole stomatal apparatus could be observed, the two subsidiary and two guard cells kept a space for outer and inner chambers (Plate III, 1–2). The subsidiary cell cuticle was the thickest, with 2.86 µm in mean, and had a high proportion of the A2 layer (81.46%) versus a thin B1 layer (18.54% of the total thickness). The guard cell cuticle was 0.34 µm thickness in mean, with 64.70% of the A2 layer and 35.30% of the B1 layer. Amorphous and darkly stained cell remnants were also present.

In many cases, the cell remnants were present, and some of the well-preserved details were observed (Plate IV). Although the cell contents, such as organelles, were not visible, cell membrane remnants were quite often present. In some cases, they were three-layered (Plate IV, 4, 7–8) as classical cell membranes, with one darkly stained and two translucent layers. In other cases, they were mono-layered (Plate IV, 1–2, 5), probably depending on the section and/or of the state of preservation; in the other photos, they were intermediate. In some cases, the cell membrane remnants make clear edges of cells (Plate IV, 1–2) or shorter parts of cells with many straight lines (Plate IV, 3–4). In some observations, they were grouped in more or less complicated foldings (Plate IV, 3, 6, 9–10), making their interpretation very difficult, as clear classical cell organelles could not be distinguished.

3.2. EDS analysis

For the EDS analysis, the present *Baiera furcata* material was compared with that of another Ginkgoales species, *Sphenobaiera huangii,* which had not been previously analyzed with EDS (Wang et al., 2005). As the most common cell cuticles available in sections mounted on grids are from ordinary epidermal cells, extremely rarely observed stomatal apparatuses were unfortunately not checked. Using the EDS system, the data of the cuticle elements that were obtained may include those from both the resin and meshes (Fig. 3). To provide only comparable values of cuticle elements, Cu, Al, Os, Si, C and O were eliminated. Among the potential ratios (Table 2, Supplementary material B), four elements (N/S, N/Cl, S/Cl, K/Ca) with insignificant differences in five measurements from the Mann–Whitney test, were selected for the two layers (A2, B1) of the ordinary epidermal cells in the lower and upper cuticles. Those with homogeneous values of resin provided similar eventual errors due to the elements in the resin. Added to the confidence interval values, all of these cuticle values were also determined to be significantly different or similar by using the Mann–Whitney test. Among the 40 possibilities of comparisons (Table 2; four ratios between A2 and B1 of the same cuticle multiplied by four types of cuticles; four ratios between A2 of the upper and lower cuticles, four ratios between B1 of the upper and lower cuticles of the same taxon multiplied by the two taxa of *Baiera* and *Sphenobaiera*; four ratios between A2 of the upper cuticles of the two taxa, four ratios between B1 of the lower cuticles of the two taxa), some had significant differences in their ratio value, while others have insignificant differences (Fig. 6). In the EDS analyses, each layer has its own characteristics.

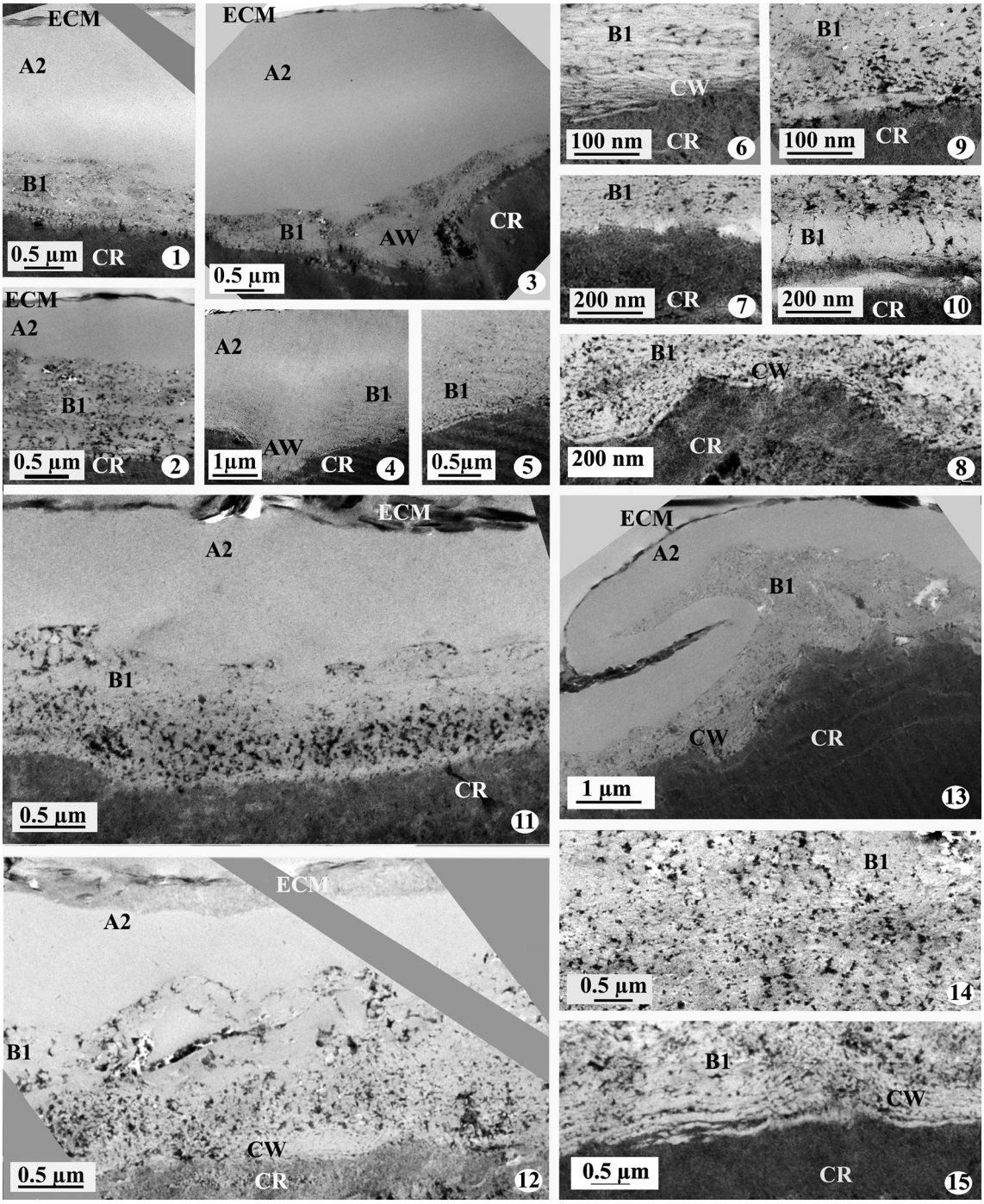

Plate II. Ultrastructural transmission electron micrographs, ordinary epidermal cell cuticles of *Baiera furcata* (specimen PB22980), details. ECM = extracuticular material, CR = cell remnants, CW = cell wall, AW = anticlinal wall, A2 = granular layer of the cuticle proper, B1 = fibrilous or reticulate layer of the cuticular layer. All micrographs are from untreated material, transversal sections. 1–10. Ordinary epidermal cell upper cuticle. 1–2. Whole cuticles with thin and thick B1 layer, respectively. Note the A2 granular layer with amorphous material, the B1 fibrilous and reticulate layer. 3–4. Cuticle areas with anticlinal walls. 5. Details of the fibrils of B1 layer of photo 4. 6–10. Details of the lower part of the cuticle, connected to the cell remnants, showing usual fibrilous and reticulate B1 layer (6–9), oriented more or less parallel to the inner surface of the cuticle. In rare cases (10), some fibrils are oriented transversely to the inner surface of the cuticle. Remnants of cell wall, with long, thin and very parallel lines are also visible in some cases. 11–15. Ordinary epidermal lower cuticle. 11–12. Two cases of whole cuticles with thin and thick B1 layer, respectively. Note the A2 granular layer with amorphous material, the B1 fibrilous and reticulate layer. In one case (12) cell wall remnants are hardly visible, made with long and thin lines very parallel to the inner surface of the cuticle. 13. Folding of the cuticle as usually observed in the lower cuticle, where the cell remnants apparently not involved in this part. Some cell wall remnants are also visible in one part. 14–15. Middle (14) and lower part (15) of the cuticle, with fibrils and reticulum of the B1 layer, directly connected to the inner surface of the cuticle or with some small fragments of cell wall remnants.

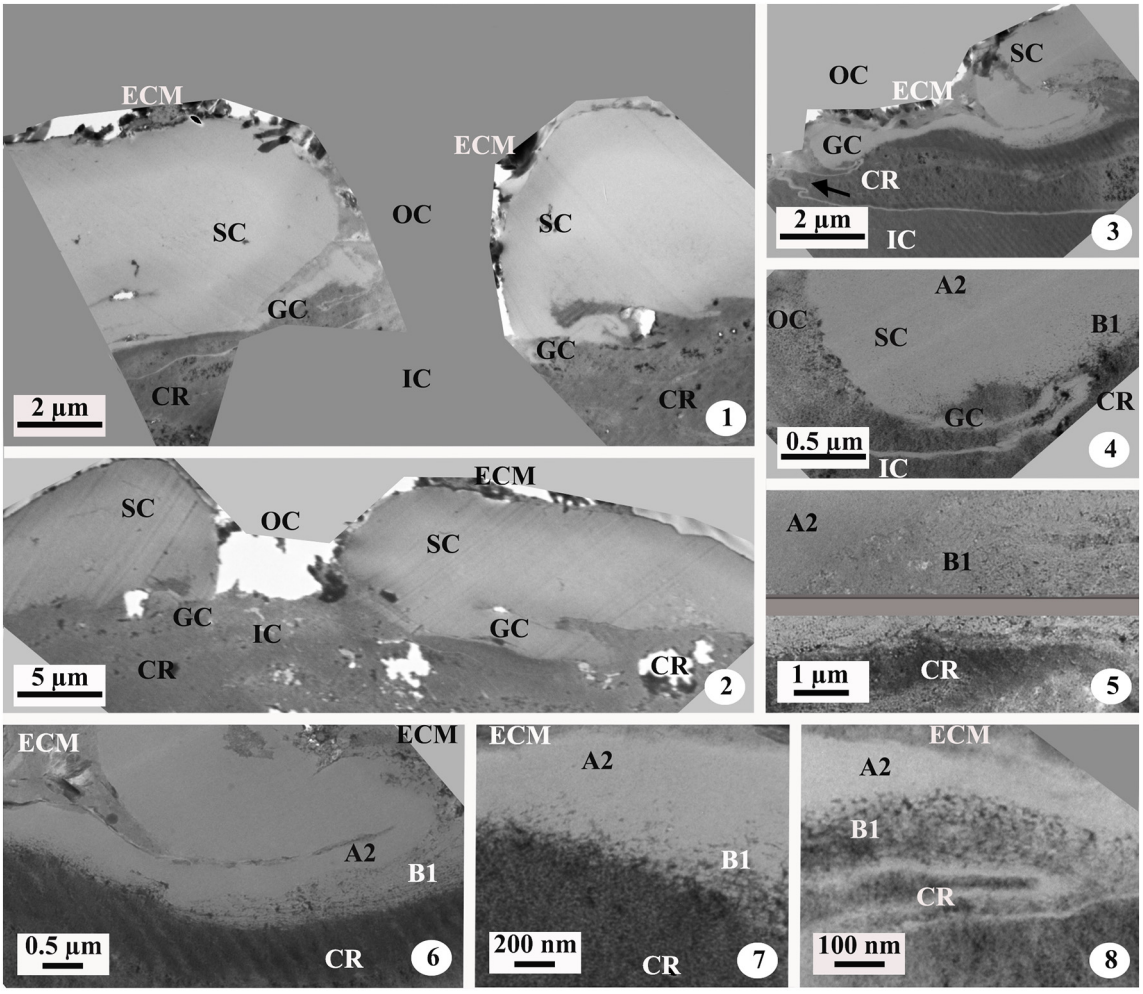

Plate III. Ultrastructural transmission electron micrographs, stomatal apparatus and subsidiary and guard cell cuticles of *Baiera furcata* (specimen PB22980). ECM = extracuticular material, CR = cell remnants, OC and IC = outer and inner chambers of the stomatal apparatus, SC and GC = subsidiary and guard cell cuticles, A2 = granular layer of the cuticle proper, B1 = fibrilous or reticulate layer of the cuticular layer. All photos are from untreated material. Except photo 1 which is from a longitudinal section, all other micrographs are from transversal sections. 1–3. General views. These whole sections provide all constituents of stomatal apparatus. Photo 3 is only half of one stomatal apparatus, with the outer and inner chambers, one guard cell and one subsidiary cell cuticles. Note the remnants of the guard cell membrane just below the cuticle (arrow). 4–5. Details of subsidiary cell cuticle, with A2 granular and B1 fibrilous and reticulate layers, the difference in consistency of the two layers being more visible in photo 5. 6–8. Details of guard cell cuticle, photos 6–7 being a detail of 3. Note the two A2 and B1 layers, directly connected to the cell remnants.

4. Discussion

4.1. Taxonomic implications

4.1.1. Ultrastructure

The present material represents the first leaf ultrastructural cuticle study on the genus *Baiera*. The result shows that the ultrastructural cuticle of *Baiera furcata* is composed of the A2 and B1 layers. Statistical measurements allowed for comparisons between different layers of the *Baiera furcata* cuticle by using the confidence interval (Fig. 4), and a three-dimensional reconstruction (Fig. 5) and a dichotomous key (Table 3) were made. By using very simple keys (Table 3), i.e., the proportions of A2 and B1 layers, as well as the total thickness of the cuticular membrane, the four types of cuticles could be identified easily. We found that subsidiary cell cuticle overlapped other cuticles that were shown to be more heterogeneous in their thickness variations. Among the three characters evaluated (total cuticular membrane [CM] thickness and thickness of A2 and B1 layers), the upper and lower cuticles of the ordinary epidermal cell and the guard cell cuticle yielded their own identities. This demonstrated the importance of the details of ultrastructural measurements and a special equilibrium for each type of cuticle.

The only other known cuticle, which is made with the A2 and B1 layers in a detailed ultrastructure, was recorded in *Sphenobaiera huangii* (Wang et al., 2005). As it also belongs to Ginkgoales, some similar characters with *Baiera furcata* are striking: this taxon is also devoid of the A1 polylamellate layer (Wang et al., 2005, figs. 19, 27); the B1 fibrilous layer is also reticulate in some cases (Wang et al., 2005, figs. 21, 33). Moreover, although the measurements for this taxon are, unfortunately, not so detailed, according to figs. 16–35 (Wang et al., 2005) the A2% and B1% of the ordinary epidermal cell upper cuticle of this taxon (76% and 24%, respectively) are quite similar with the present material of *Baiera* (72.24% and 27.76%, respectively).

Although the number of studies is still too limited in Gingkoales, based on the present material, it seems that this order may be composed of two ultrastructural groups of cuticles: the *Baiera–Sphenobaiera* type (two taxa: *Baiera furcata, Sphenobaiera huangii*) is made with A2 and B1 layers, while the *Ginkgo–Ginkgoites–Pseudotorellia* type (six taxa: living *Ginkgo biloba,* fossils *Ginkgo yimaensis*, *Ginkgoites ticoensis*, *G. skottbergii*, *Pseudotorellia asiatica* Nosova et Kiritchkova and *P. samylinae* Nosova et Kiritchkova) has a very different cuticle, with A1 upper and lower sublayers, A2 and B1 layers (Guignard and Zhou, 2005; Del Fueyo et al., 2006, 2013; Guignard et al., 2016; Nosova et al., 2019). For *Ginkgoites*, *G. tigrensis* Archang. (Villar de Seoane, 1997)

Table 1
Statistical values, made with 30 measurements for each type of cell cuticles of *Baiera furcata*.

Ordinary epidermal cell, upper cuticle					Ordinary epidermal cell, lower cuticle			
	Mean	Min–max	%	St-d	Mean	Min–max	%	st-d
CM	2.63	2.08–3.94	100	0.57	1.53	1.13–1.92	100	0.23
CP (A)	1.90	1.16–3.13	72.24	0.49	0.67	0.29–1.17	43.79	0.22
A2	1.90	1.16–3.13	72.24	0.49	0.67	0.29–1.17	43.79	0.22
CL(B)	0.72	0.33–1.62	27.76	0.37	0.86	0.53–1.25	56.21	0.20
B1	0.72	0.33–1.62	27.76	0.37	0.86	0.53–1.25	56.21	0.20
Stomatal apparatus								
Subsidiary cell cuticle					Guard cell cuticle			
	Mean	Min–max	%	St-d	Mean	Min–max	%	St-d
CM	2.86	0.3–5.02	100	1.79	0.34	0.20–0.56	100	0.11
CP (A)	2.33	0.23–5.02	81.46	1.7	0.22	0.09–0.39	64.70	0.08
A2	2.33	0.23–5.02	81.46	1.7	0.22	0.09–0.39	64.70	0.08
CL (B)	0.53	0–2.30	18.54	0.69	0.12	0.05–0.31	35.30	0.08
B1	0.53	0–2.30	18.54	0.69	0.12	0.05–0.31	35.30	0.08

Note. Min–max = minimum and maximum values observed. % = percentage of each detailed part of the cuticle. st-d = standard deviation. The cuticular membrane CM is made up with cuticle proper CP (=A = A2 layer) and cuticular layer CL (=B = B1 layer). All measurements are in μm.

were shown without a detailed ultrastructure but had a cuticle assigned to Karkeniaceae with strong affinities to the two layers of *Sphenobaiera huangii* (Wang et al., 2005), which is not considered in this paper. It is interesting to note that, from our study, Ginkgoales are divided into two ultrastructural groups, while in gross morphology, there are more than two groups of leaf fossils (Zhou, 2009): *Ginkgo* and *Ginkgoites* are more or less related; *Baiera* and *Sphenobaiera* are different. At present, there is only one known species of each *Baiera* and *Sphenobaiera* that have been studied at the species level of taxonomy; thus, only the potential genus-species taxonomy level can be evocated. Four characters can be summarized: (1) *S. huangii* has the same thickness for both upper and lower ordinary epidermal cell cuticles (6.5 μm), showing a difference with that of *B. furcata* (2.63 and 1.53 μm, respectively). (2) The subsidiary cell cuticle is slightly thinner than the ordinary epidermal cell cuticle in *S. huangii* (6 μm versus 6.5 μm, respectively), which is contrary to that in *B. furcata* (2.86 versus 2.63 μm, respectively). (3) The guard cell cuticle is approximately three times thinner than the ordinary epidermal cell cuticle in *S. huangii* (2.5 for 6.5 μm, respectively) and is approximately nine times thinner in *B. furcata* (0.34 versus 2.63 μm, respectively). (4) The percentages of the thickness of the A2 layer of the subsidiary and guard cell cuticles are smaller than the B1 layer in *S. huangii* (8.33% and 32% versus 91.66% and 68%, respectively), which is the reverse in *B. furcata* (64.7% and 81.46% versus 18.54% and 35.3%, respectively). Compared with other taxonomical groups, no other fossil families or orders are identical to the present *Baiera furcata* ultrastructural features of cuticle; they are Czekanowskiales (Zhou and Guignard, 1998), Pteridospermales (Guignard et al., 2001; Thévenard et al., 2005; Carrizo et al., 2014), including Corystospermaceae (Guignard et al., 2004), Bennettitales (Villar de Seoane, 1999, 2001, 2003); cycadalean cuticles (Artabe et al., 1991; Archangelsky et al., 1995; Passalia et al., 2010), Coniferales Cheirolepidiaceae (Guignard et al., 1998; Yang et al., 2009; Guignard et al., 2017; Yang et al., 2018) and Miroviaceae (Nosova et al., 2016), living Pinaceae (Bartiromo et al., 2012).

Due to good preservation of the material, the guard cell cuticle is present and noticeable, although it is not so often observed by TEM. The low thickness of the guard cell cuticle, which is usually observed in many taxa, is usually correlated with the function of closing or opening the stoma, as a thin cuticle is much more malleable than a thick cuticle. The guard cell cuticle was revealed to be the thinnest of the other types of cuticles of *Baiera*, with 0.34 μm in average thickness versus 2.63 and 1.53 μm in the mean for the two ordinary epidermal cell cuticles (Table 1). In the group *Baiera–Sphenobaiera*, the latter taxon *Sphenobaiera* shows a thinner guard cell cuticle (2.5 μm versus 6.5 for the two ordinary epidermal cell cuticles) (Wang et al., 2005); therefore, we can state the homogeneity of this group. It seems to be different for the group *Ginkgo–Gingkoites–Pseudotorellia*, for which two possibilities occur. The fossil *Ginkgoites* agrees with the taxa just evocated: *G. ticoensis* has 0.46 μm in mean thickness for the guard cell cuticle, 1.02 μm for the ordinary epidermal cell cuticle (Del Fueyo et al., 2013); in *G. skottsbergii* (Guignard et al., 2016), the guard cell cuticle is 0.47 μm and the ordinary epidermal cell cuticle is 2.07 μm. However, as a contrary, the *Ginkgo* (living *G. biloba* male and female, fossil *G. yimaensis*), guard cell cuticle is thicker than all lower cuticles, with 1.76–2.34 μm for the guard cell cuticle, 1.11–1.75 μm for the 3 lower ordinary epidermal cell cuticles (Guignard and Zhou, 2005). These *Ginkgo* guard cell cuticle features are very unusual, as guard cell cuticles are also very thin in other taxa beside Ginkgoales: in Cheirolepidiaceae, *Pseudofrenelopsis dalatzensis* (Chow et Tsao) Cao ex Zhou, *Pseudofrenelopsis gansuensis* Deng, Yang et Lu, the guard cell cuticle is 1.77–1.88 μm thick, and the ordinary epidermal cell cuticles are 9.41–12.27 μm (Yang et al., 2009; Guignard et al., 2017); in *Hirmeriella muensteri* (Schenk) Jung, the guard cell cuticle is 0.8 μm thick, and the ordinary epidermal cell cuticle is 11.5 μm (Guignard et al., 1998). In Pteridospermales (*Dichopteris*), the guard cell cuticle is 3.6 μm thick, the ordinary epidermal cell cuticle is 14.7–17.8 μm (Thévenard et al., 2005). In pteridosperms, *Pachypteris* leaves have a guard cell cuticle of 3.99 μm in thickness and an ordinary epidermal cell cuticle of 13.68–12.26 μm thick (Guignard et al., 2004). In some living plants, such as *Agave americana* L., *Plantago major* L. and *Ardisia crenata* Sims, the A1 polylamellate layer is correlated with impermeability (Fischer and Bayer, 1972; Wattendorff and Holloway, 1980, 1982; Wattendorff, 1992; Jeffree, 2006). The present fossil guard cell cuticle is, therefore, quite unusual compared with most of the other fossil guard cell cuticles. *Baiera furcata* has the same layers as the ordinary epidermal and subsidiary cell cuticles, A2 and B1. In some living angiosperms, such as *Agave Americana, Plantago major* and *Ardisia crenata*, the A1 polylamellate layer is correlated with impermeability (Fischer and Bayer, 1972; Wattendorff and Holloway, 1980, 1982; Wattendorff, 1992; Jeffree, 2006). As A1 is absent from the present material, the impermeability of the guard cell cuticle could be related in this case with the presence and special thickness % equilibrium of the A2 and B1 layers (approximately 2/3 of A2 and 1/3 of B1 layers; Table 1).

4.1.2. EDS

In our study, approximately six-element and four-element EDS ratios were selected (N/S, N/Cl, S/Cl, K/Ca, Supplementary material B); thus, different types of comparisons can be achieved. It has to be noticed, first, that this study reveals the same range of ratios as those of former EDS studies, with three-five ratios and four-five elements selected: N/F, N/Cl, F/Cl, K/Ca in Coniferales, Cheirolepidiaceae, *Suturovagina intermedia* (Yang et al., 2018); N/S, N/Cl, N/K in Coniferales, Cheirolepidiaceae, *Pseudofrenelopsis dalatzensis* and *P. gansuensis* (Guignard et al., 2017); Cl/N, K/S, N/Ca, S/Ca, K/Ca in Gingkoales, *Ginkgoites ticoensis* and *G. skotttsbergii* (Guignard et al., 2016). Comparing the present EDS results with those of former studies, the N/Cl (or Cl/N) ratio seems to be characteristic of cuticles of all orders and is, therefore, always significant.

For fossil plants, the EDS data are very limited and are only available for very few taxa. Thanks to TEM EDS, details of the elements of the different cuticle layers are, therefore, possible for taxonomical considerations. Some cuticle part may show element differences of distinction between genera or species, e.g., in gymnosperms (D'Angelo et al., 2010), seed ferns, conifers and cycad-related fossils (D'Angelo and Zodrow, 2011; D'Angelo et al., 2011); pteridophyll cuticles (Zodrow and Mastalerz, 2007); or other seed ferns (Zodrow et al., 2010; D'Angelo et al., 2012). It is also the case in chemotaxonomy for N and Cl (tree ferns in Stoyko et al., 2013) and N, Ca, Cl (seed ferns in

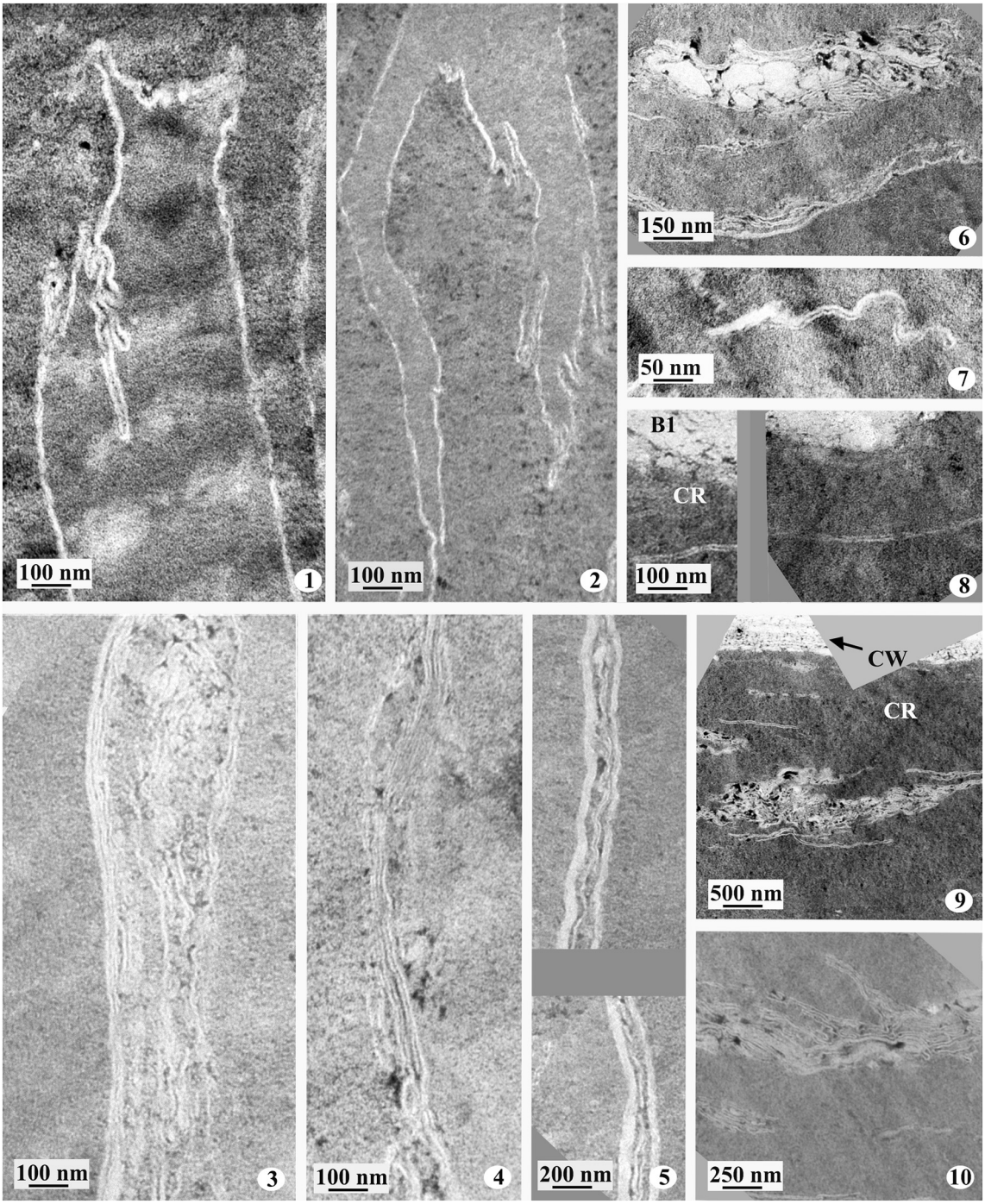

Plate IV. Ultrastructural transmission electron micrographs, cell remnants of *Baiera furcata* (specimen PB22980). All micrographs are from untreated material, transversal sections. CR = cell remnants, CW = cell wall, B1 = fibrilous or reticulate layer of the cuticular layer. 1–2. Edges of cells with cell membranes remnants mono-layered in these two cases. 3–5. Long parts of cells with straight cell membranes three-layered in some parts, mono-layered in other parts. Between these straight membranes, other more or less agglomerated membranes may also occur as in photo 3. 6–10. More or less agglomerated membranes, three- or mono-layered, among amorphous cell remnants. In the upper part of photo 6 amorphous translucent material mixed with membranes is also observed.

Zodrow et al., 2016). Based on the present and former EDS studies (Guignard et al., 2016), for Ginkgoales, K/Ca is useful for all studied taxa and could be a potential order characteristic; however, it is not exclusive, as it is also useful for one genus of Coniferales, *Suturovagina* belonging to Cheirolepidiaceae (Yang et al., 2018). Within Ginkgoales, the two groups *Baiera–Sphenobaiera* and *Ginkgo–Ginkgoites,* just evocated in their ultrastructure, are also congruent. *Sphenobaiera huangii* (Wang et al., 2005) could be used for EDS comparisons using the Mann–Whitney test; these element analyses are also significant for the group *Baiera–Sphenobaiera,* as it shows two significant EDS common ratios (Fig. 6, Table 2 middle part), including N/Cl, K/Ca for B1 of both lower cuticles. Moreover, the other group of Ginkgoales (*Ginkgo–Ginkgoites*), shows very different EDS ratios, based on an unfortunate few study cases of EDS in one genus (*Ginkgoites*) (Guignard et al., 2016). Ultrastructurally, only one species of each *Baiera* and *Sphenobaiera* were studied in EDS until now; thus, only the genus-species taxonomy level can be summarized. At this level, three points can be evocated. First, comparing *Baiera furcata* and *Sphenobaiera huangii* cuticles (Table 2, middle part), predominant and significant differences were recognized and enhance the identity of each taxon at the genus-species level.

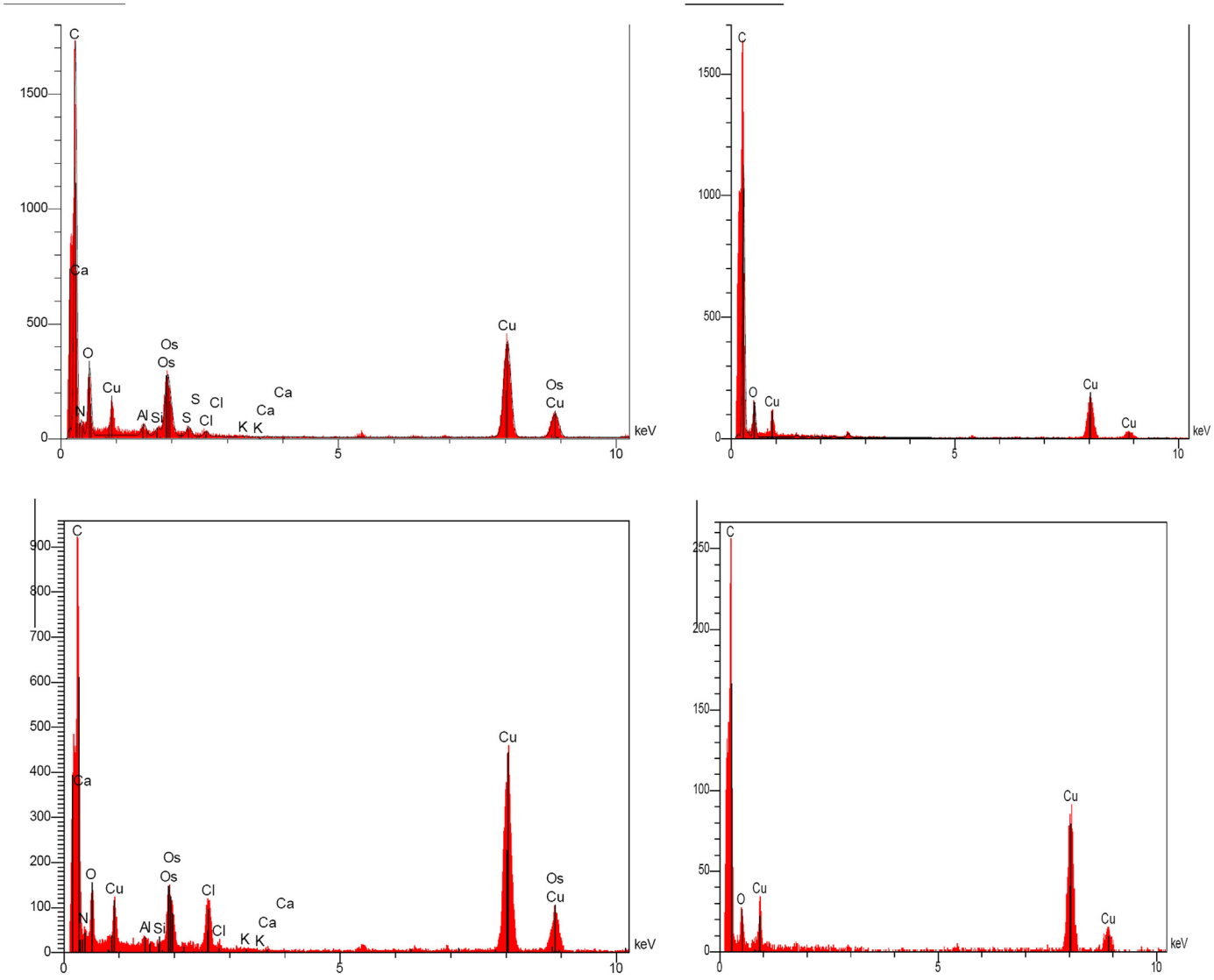

Fig. 3. Examples of EDS analyses of *Baiera furcata* and *Sphenobaiera huangii* cuticles and resins. For each taxon (a, b), the A2 lower cuticles diagrams are on the left side, the resin diagrams on the right side.

Among all ratios, eight of them seem to be of potential genus-species taxonomical interest, as they are significantly different between the two taxa (Table 2: N/S, N/Cl, S/Cl, K/Ca for both A2 upper and lower cuticles; N/S, S/Cl for both B1 upper and lower cuticles; N/Cl, K/Ca for B1 upper cuticles). Second, the details of the A2 and B1 layers in *Baiera furcata* are totally homogeneous in both the upper and lower cuticles

Table 2
Summary of EDS ratios significant differences or/not between the layers of *Baiera furcata* and *Sphenobaiera huangii* upper and lower cuticles.

types of Mann-Whitney tests		between A2 or between B1 of the 2 cuticles of *Baiera furcata*		between A2 or between B1 of the 2 cuticles of *Sphenobaiera huangii*		between A2 or between B1 of the two taxa, for OEC upper cuticle		between A2 or between B1 of the two taxa, for OEC lower cuticle			between A2 and B1 of the 2 cuticles of *Baiera furcata*		between A2 and B1 of the 2 cuticles of *Sphenobaiera huangii*	
layers	**ratios**	**OEC upper cuticle**	**OEC lower cuticle**	**OEC upper cuticle**	**OEC lower cuticle**	***Baiera furcata***	***Sphenobaiera huangii***	***Baiera furcata***	***Sphenobaiera huangii***	**layers and ratios**	**OEC upper cuticle**	**OEC lower cuticle**	**OEC upper cuticle**	**OEC lower cuticle**
A2	**N/S**	0.29-0.31		1.26	0.85	0.31	1.26	0.29	0.85	**A2 N/S**	0.31	0.29-	1.09-1.26	0.85-1.58
										B1 N/S		0.33		
A2	**N/Cl**	0.92	0.42	0.09	0.05	0.92	0.09	0.42	0.05	**A2 N/Cl**	0.78-	0.39-	0.07-0.09	0.05
A2	**S/Cl**	2.93	1.51	0.07		2.93	0.07	1.51	0.07	**B1 N/Cl**	0.92	0.42		0.56
A2	**K/Ca**	1.18-1.44		0.83	0.44	1.18	0.83	1.44	0.44	**A2 S/Cl**	2.58-	1.16-	0.06-0.07	0.07-0.49
B1	**N/S**	0.31-0.39		1.09-1.58		0.31	1.09	0.33	1.58	**B1 S/Cl**	2.93	1.51		
B1	**N/Cl**	0.78	0.39	0.07	0.56	0.78	0.07	0.39-0.56		**A2 K/Ca**	1.11-	1.44-	0.46-0.83	0.44
										B1 K/Ca	1.18	1.84		1.08
B1	**S/Cl**	2.58	1.16	0.06-0.49		2.58	0.06	1.16	0.49					
B1	**K/Ca**	1.11-1.84		0.46-1.08		1.11	0.46	1.08-1.84						

Note: green color = insignificant differences, the 2 means are indicated for each ratio; purple color = significant differences, each mean is indicated for each ratio.

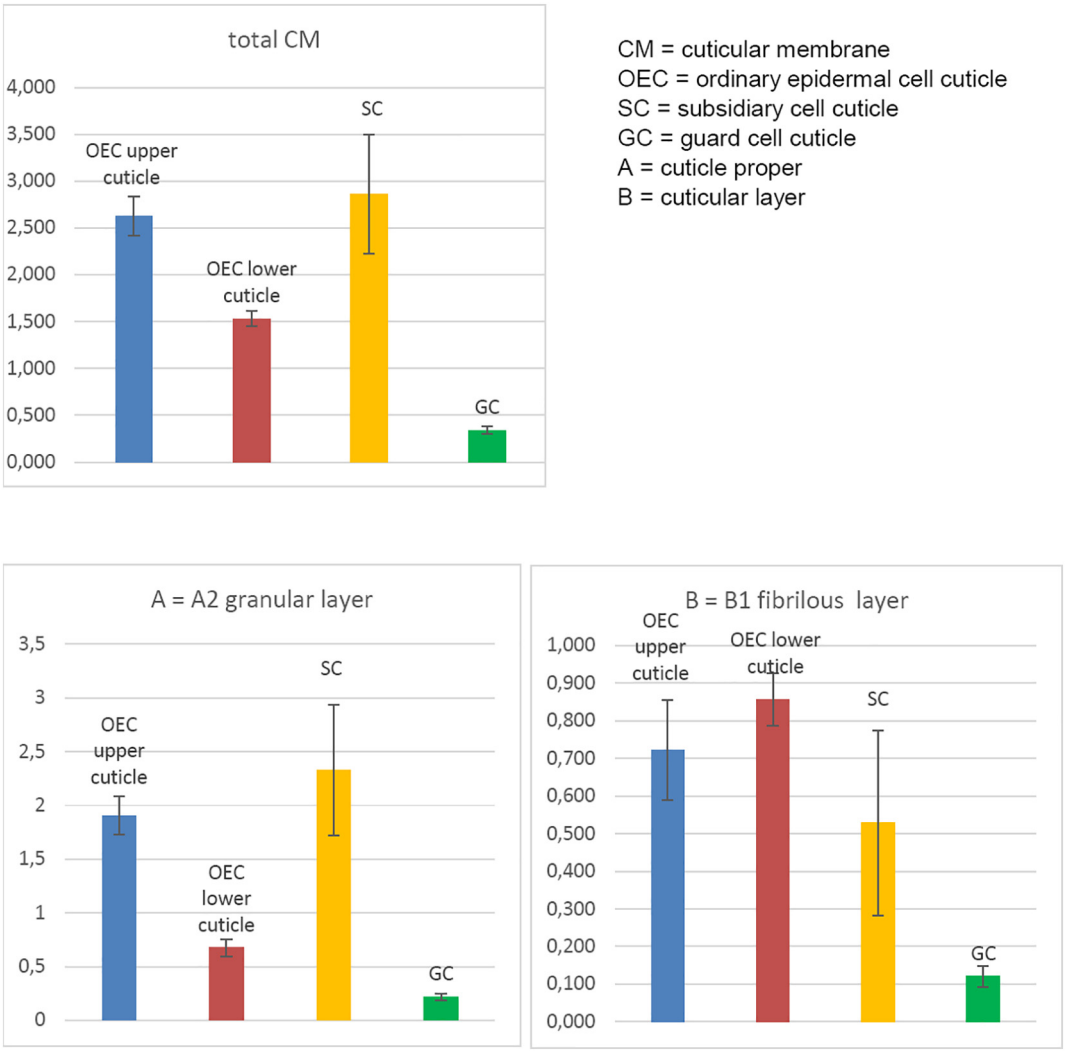

Fig. 4. Means and confidence intervals of the layers of *Baiera furcata* upper and lower cuticles.

(Table 2, right part). This demonstrates the unity of these cuticles in their element compositions. It shows almost the same schemes for *Sphenobaiera,* with 100% homogeneity for the upper cuticle; however, its lower cuticle shows half heterogeneity between the A2 and B1 layers. Third, comparing the two A2 layers (or the 2 B1 layers) between the upper and lower cuticles (Table 2 left part), half of the ratios are significantly different, showing the identity of each upper and each lower cuticle in *Baiera furcata*. This is also the same scheme for *Sphenobaiera huangii,* but with different ratios. The insignificant characteristics are homogeneous but show the identity of each taxon. Differences between upper and lower cuticles of one taxon are difficult to interpret; however, the different and possible roles of these two parts of a leaf may be evocated for these different molecular compounds.

Although cell organelles seem to be absent from the present material, the quality of cell residues with distinct membranes is quite interesting, as cell remnants are mostly found in younger geological periods and mainly in angiosperms (Niklas et al., 1978; Niklas and Brown, 1981; Niklas, 1983; Niklas et al., 1985; Schoenhut et al., 2004; Shen et al., 2016). However, in recent years, they have been increasingly observed in Mesozoic gymnosperms, i.e., Ginkgoales (Del Fueyo et al., 2013) and Coniferales (Guignard et al., 1998; Yang et al., 2018). This enhances the very good quality of the present *Baiera* fossils, as they were found in gray mudstone which allowed this excellent preservation. In this good preservation, the membrane three-layered were observed in some places, similar with living plants membranes. However, organites like chloroplasts could not be found, it seems that these organites are much more preserved in fossil plants from younger geological periods, and vanished in older material. Cell remnant ratios of the present material could not be compared with those of *Sphenobaiera huangii,* as they were absent from the latter material; however, the EDS ratio values and Mann–Whitney test (Supplementary material C) show significant differences among the cuticle ratios and demonstrate the real identity of this material. Although ratios of cuticle layers are variable, for *Baiera* cell remnants N/S (0.57) is always higher than for cuticle layers, N/Cl (0.90) is higher except for one value of A2 from upper cuticle (0.92), S/Cl is among the values of cuticle layers, K/Ca is always lower. This conducts to a tendency for more N, K, Cl in cell remnants than in cuticle layers, conversely for less S and Ca.

4.2. Paleoenvironment

Interestingly, three complementary aspects can be envisaged: the cuticle TEM and EDS details, the EDS of the rock matrix, and the associated flora of the two taxa are compared.

First, the function of molecules in the cuticles is mainly studied in some living angiosperm taxa (Fernández and Eichert, 2009; Dominguez et al., 2011; Fernández and Brown, 2013). However, there are still very few cuticle results on the elements, and the “chemical uptake behavior of leaves… remains largely unknown” (Ahmadi et al., 2016). No result had yet been obtained by using the details of the

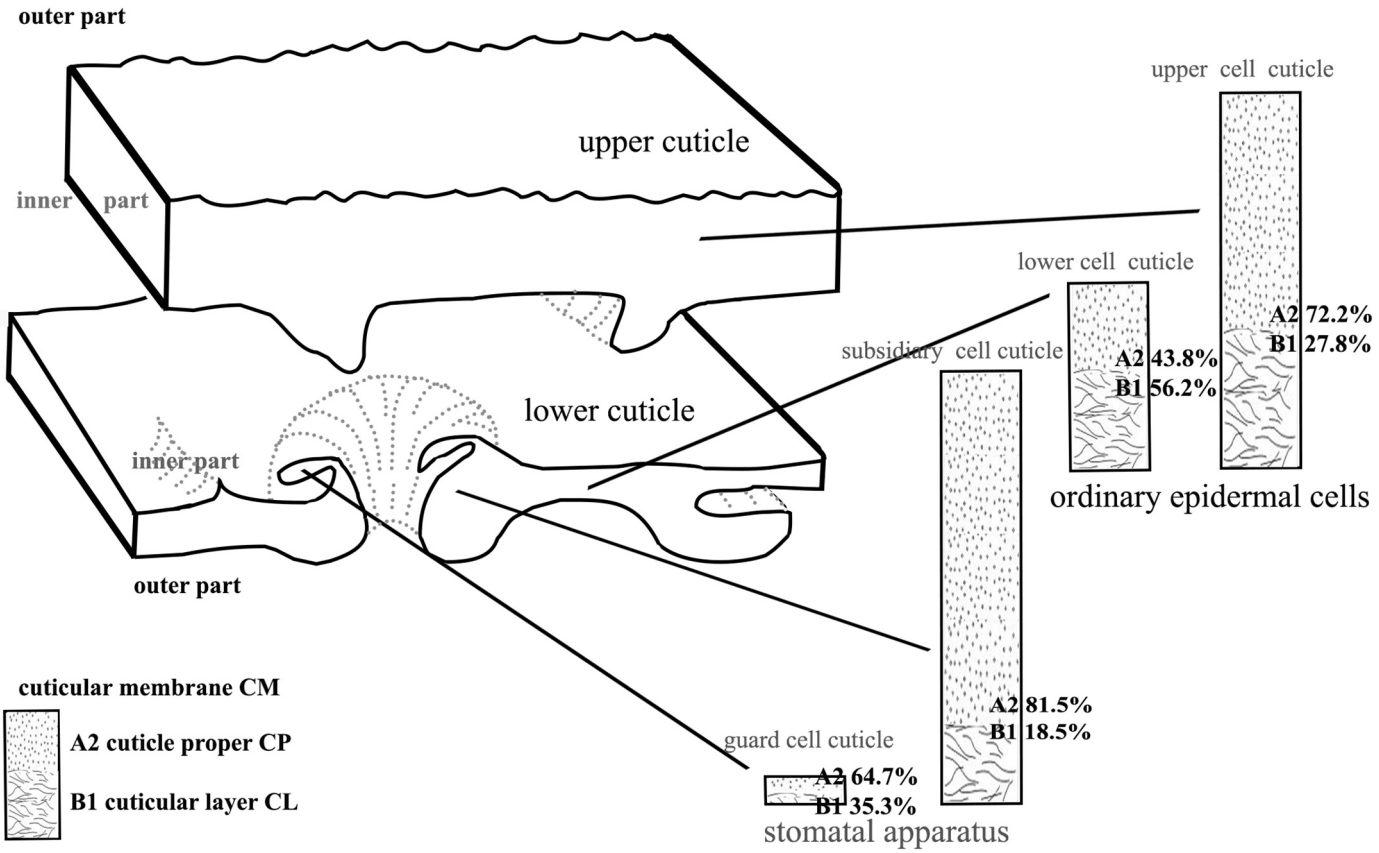

Fig. 5. Three-dimensional reconstruction of the cuticles of *Baiera furcata* with TEM ultrastructure.

different cuticle layers, as was achieved successfully for the present fossil material. Concerning environmental considerations and TEM results, the previous comparisons between the same species from two different environments demonstrated the influence on the layers of cuticles (fossil *Komlopteris nordenskioeldii* (Nathorst) Barbacka, Guignard et al., 2001; living *Pinus halepensis* Mill. and living *Erica arborea* L., Bartiromo et al., 2012, 2013). Moreover, EDS was recently applied efficiently to fossil *Suturovagina intermedia* Chow et Tsao (Yang et al., 2018), and some element ratios were evaluated for the environmental signature. It was significantly different between two paleoenvironments (more and less xerothermic) for the same species. In this study, we include two species of two genera; it is, thus, not evident to demonstrate the influence of the environmental significances. However, in comparison with the *Suturovagina* study, some convergent remarks can be made. This enhances the possible signature of the paleoenvironment through the cuticle details, which indicate warmer climate for *Sphenobaiera huangii* than for *Baiera furcata*.

Five EDS elements were used efficiently for this study (S, N, K, Ca, Cl). However, although the first two elements were studied based on the cuticles and environment in other living and fossil plants (Grammatikopoulos et al., 1998; Santrucek et al., 2004; Guan et al., 2011; Rashidi et al., 2012; Elliott-Kingston et al., 2014; Fernández et al., 2016; Somapala et al., 2016; Simioni et al., 2017; Steinthorsdottir et al., 2018), only the last three elements (Ca, K, Cl) seemed to infer potential interest for the paleoenvironment in the present study. The thickness of the cuticle of *Baiera furcata* is less thin (over two times thinner: ordinary epidermal cell cuticles are 2.63 and 1.53 μm in mean, for the upper and lower cuticles, respectively; and 6.5 μm in average for both upper and lower cuticles in *Sphenobaiera huangii*, Wang et al., 2005), which is usually related to a less xerothermic environment. In addition, two EDS results or data also converged for the same considerations. First, potassium (K) is useful in plant cuticle development (genera *Agave* and *Clivia*, Wattendorff and Holloway, 1982), and its penetration through the cuticle is studied in angiosperms (Schönherr, 2002; Elshatshat et al., 2007), especially in *Pyrus* and *Citrus* (Schönherr and Luber, 2001), as well as in *Acer* and *Citrus* (Tyree et al., 1990). More precisely with xerothermy and stress, Ca is also well studied in cuticles (Guzmán-Delgado et al., 2016), and in a study of leaves of living *Arabidopsis thaliana* (L.) Heynh., Benikhlef et al. (2013) experimented with "a soft mechanical stimulation" to induce an artificial "stress" that is related to a higher Ca content. In the fossil *Suturovagina* study, a higher K/Ca ratio (= lower Ca value) was potentially related to a lower xerothermy (Yang et al., 2018). In the present study, compared with *Sphenobaiera huangii,* the K/Ca values are always higher in *Baiera furcata* (Table 2), which may induce a possible climate that is less warm for the *Sphenobaiera* taxon. Second, following the study in living *Pinus ponderosa* Lawson and *Pseudotsuga menziesii* (Mirb.) Franco, where the cuticular transpiration is revealed to be higher during

Table 3
Dichotomous key for the four types of cuticles of *Baiera furcata*.

	Total cuticle thickness 0.3 μm	65% A2 versus 35% B1		Guard cell cuticle
Thicker A2 than B1 layer	Total cuticle thickness 2.6–2.9 μm	81% A2 versus 19% B1	Total cuticle thickness 2.86 μm	Subsidiary cell cuticle
		72% A2 versus 28% B1	Total cuticle thickness 2.63 μm	Ordinary epidermal cell upper cuticle
Thicker B1 than A2 layer	44% A2 versus 56% B1		Total cuticle thickness 1.5 μm	Ordinary epidermal cell lower cuticle

Note. The total thickness of the cuticular membrane may be divided in two components: A2 of the cuticle proper and B1 of the cuticular layer.

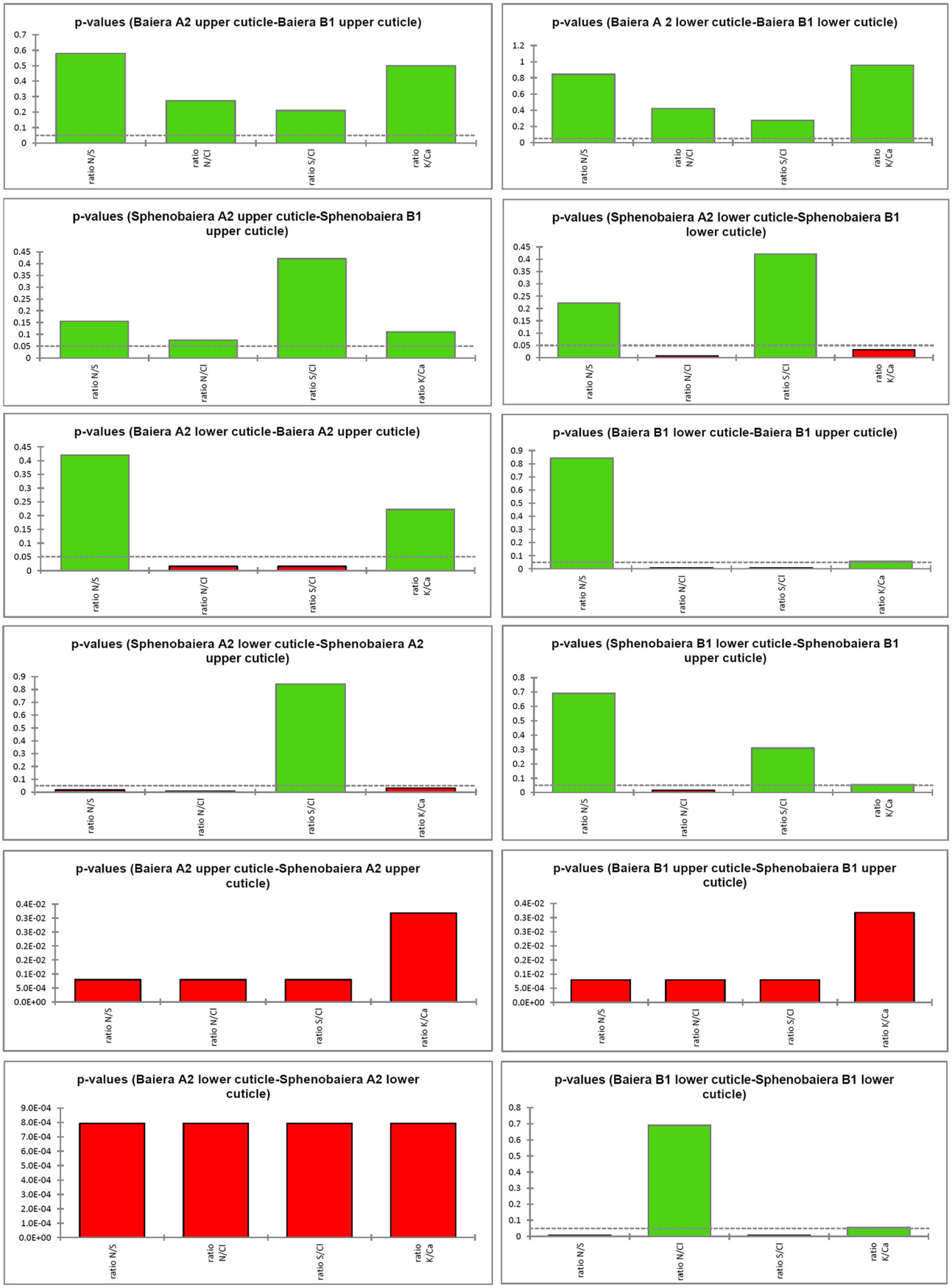

Fig. 6. Mann–Whitney p-values of the EDS differences or/not between the layers of the cuticles of *Baiera furcata* and *Sphenobaiera huangii*.

exposure to chlorine gas (Schreuder and Brewer, 2001), a lower concentration of Cl was possibly related to a lower xerothermy in *Suturovagina*. As all ratios with Cl seem to indicate a lower Cl concentration for the present *Baiera furcata* study (original values are 2.16–3.28%) compared with *Sphenobaiera huangii* (original values are 2.91–15.06%), it may indicate a lower potential transpiration, although a less warm climate for *Baiera furcata* may be inferred.

Second, comparing the EDX matrix sediment analysis, although the data are quite heterogeneous (Supplementary material D), a higher C content for *Baiera* sediments (6.85–63.06%, present in each of the six checks) and a lower C content for *Sphenobaiera* sediments (4.74–10.63%, only present in three of the five checks) were observed. These kinds of values were formerly enhanced for a difference in the xerothermy between the two localities of *Suturovagina* (Cheirolepidiaceae, Yang et al., 2018), which agreed with a possibly less warm climate for *Baiera* and a warmer climate for *Sphenobaiera*. In the *Suturovagina* localities, a lower Ca content was associated with a lower xerothermy versus a higher Ca content associated with a higher xerothermy; however, it is contrary in the present case, as for *Baiera* sediments, the values were 0.46–6.28%, while they were 0.21% for *Sphenobaiera*.

Third, in the Huolinhe Formation, the present *Baiera furcata* was found to be associated with *Ginkgo coriacea* Florin, *Sphenobaiera ikorfatensis* (Seward) Florin, *Phoenicopsis angustifolia* (Heer) Samylina, *Phoenicopsis (Culgoweria) huolinhensis* Sun and *Czekanowskia* sp. (Sun, 1987, 1993; Sun et al., 1995; Sun et al., 2003); all were typical temperate or warm temperate elements in the Siberian-Canadian floristic region (Vachrameev, 1991; Sun, 1993). The fossil plants from the Early Cretaceous Huolinhe Formation have 69 species belonging to 36 genera, including 28 species of ferns, 11 species of Cycadopsida, 8 species of Ginkgoales and 13 species of Coniferopsida (Deng, 1995). The abundant plants in the Huolinhe Formation might indicate that a warm or moderate climate dominated this area during the Early Cretaceous. Except for the flora mentioned above, there are five fossil conifer woods reported in the Huolinhe Formation, including *Phyllocladoxylon eboracensee* (Holden) Krausel, *Podocarpoxylon dacrydioides* Cui, *Protocedroxylon orientale* He, *Xenoxylon huolinhense* Ding and *Xenoxylon peideense* Zhang et Zhang(Cui, 1995; He, 1995; Yang et al., 2013). It is of interest to see that all these woods have distinct growth rings. Therefore, the climate at the time Early Cretaceous in eastern Inner Mongolia was warm-temperate, humid and seasonal. Concerning *Sphenobaiera huangii*, the presence of more tropical plants, such as ferns (*Marattia* of Mattoniaceae; Wang, 2002), *Phlebopteris* of Matoniaceae (Wang and Mei, 1999) and scale-like leaf conifers (*Brachyphyllum* specimens from new collection in this locality), seem to indicate a warmer climate rather than that of the *Baiera* locality.

5. Conclusions

In the ultrastructure, each of the four cuticles of *Baiera furcata* (ordinary epidermal cell upper and lower cuticles, subsidiary and guard cell cuticles of the stomatal apparatus) was made with an A2 layer of the cuticle proper and a B1 layer of the cuticular layer. Each cuticle has its own characteristics, besides an overlapping of the thickness and high variability of subsidiary cell cuticles overlapping the other three cuticles. The guard cell cuticle is the thinnest of the cuticles, and cell remnants made with cell membranes show the very good quality of preservation of the material. Compared mainly with another Ginkgoales species, *Sphenobaiera huangii,* which has the same type of cuticle, it seems that within this order, two groups of cuticles are potentially emerging: one group (*Baiera–Sphenobaiera*) with A2 and B1 layers, and the other group (*Ginkgo–Ginkgoites–Pseudotorellia*) with A1U and A1L sublayers, A2 and B1 layers. In the ultrastructure, the comparisons between the two taxa allow some characteristics to be enhanced at the potential genus–species level: the same thickness or different thickness between the two upper and lower ordinary epidermal cell cuticles; thinner or thicker subsidiary or guard cell cuticles compared with ordinary epidermal cell cuticles; a reversed % of thickness of A2 and B1 layers for both subsidiary and guard cell cuticles. Thanks to EDS element analysis, the present material could be compared with data on *Sphenobaiera huangii* and with data on *Ginkgoites*. Although the number of studied taxa is still too low, taxonomically speaking, the K/Ca ratio could be characteristic of the order Ginkgoales. The ratios allow for a distinction between two genera groups, *Baiera–Sphenobaiera* and *Ginkgo–Ginkgoites*. *Baiera–Sphenobaiera* is distinct with two common ratios; in this group for each taxon, eight ratios seem to be of interest for the genus-species level. There is a majority of unity of the EDS elements among the two layers for each taxon; there is also an identity of the upper and lower cuticles for each taxon. As in the TEM studies, Ginkgoales are divided into two ultrastructural groups, while in gross morphology, there are more than two groups; these new findings should be more developed among more than five genera that have been studied until now. A higher number of studied genera in the ultrastructure would certainly provide new insights and a more synthetic view of Ginkgoales. Although comparisons have to make with caution, as they concern two materials from two different genera, according mainly to two main EDS comparisons among Ca, K and Cl, a paleoenvironmental signature with the fine details of the cuticles seems to draw warmer conditions for *Sphenobaiera huangii* with a thicker cuticle, compared with the thinner cuticle of *Baiera furcata*. These paleoenvironmental considerations seem to be in congruence with associated flora and EDX elements of matrix sediments.

Acknowledgments

The study was supported by the National Natural Science Foundation of China (Grant Nos. 41472011, 41688103, 41790454), and the Strategic Priority Research Program (B) of the Chinese Academy of Sciences (Grant No. XDB1800000). We thank Dr. Georgina Del Fueyo and two anonymous reviewers for their helpful criticism and improvement of the present manuscript. We wish to thank the technical staff of the University Lyon 1 «centre technologique des microstructures CTμ," especially Xavier Jaurand and Veronica La Padula for improvement of the study.

Appendix A. Supplementary data

Supplementary data to this article can be found online at https://doi.org/10.1016/j.revpalbo.2019.05.006.

References

Ahmadi, H., Bolinius, D.J., Jahnke, A., MacLeod, M., 2016. Mass transfer of hydrophobic organic chemicals between silicone sheets and through plant leaves and low-density polyethylene. Chemosphere 164, 683–690.

Archangelsky, S., Del Fueyo, G., 1989. *Squamastrobus* gen n, a fertile Podocarp from the Early Cretaceous of Patagonia, Argentina. Rev. Palaeobot. Palynol. 59, 109–126.

Archangelsky, S., Taylor, T.N., 1986. Ultrastructural studies of fossil plant cuticles. II. *Tarphyderma gen. n.*, a Cretaceous conifer from Argentina. Am. J. Bot. 73, 1577–1587.

Archangelsky, S., Taylor, T.N., Kurmann, M.H., 1986. Ultrastructural studies of fossil plant cuticles: *Ticoa harrisii* from the early Cretaceous of Argentina. Bot. J. Linn. Soc. Lond. 92, 101–116.

Archangelsky, A., Andreis, R., Archangelsky, S., Artabe, A., 1995. Cuticular characters adapted to volcanic stress in a new Cretaceous cycad leaf from Patagonia, Argentina. Considerations on the stratigraphy and depositional history of the Baqueró Formation. Rev. Palaeobot. Palynol. 89, 213–233.

Artabe, A.E., Zamuner, A.B., Archangelsky, S., 1991. Estudios cuticulares en cycadópsidas fósiles. El género *Kurtziana Frenguelli* 1942. Ameghiniana 28, 365–374.

Barale, G., Baldoni, A., Samuel, E., 1992. Etude de la cuticule des feuilles de Podocarpacées du Crétacé inférieur de la Formation Baqueró(Argentine): Observation en microscopie photonique: électronique à balayage et à transmission. Courier Forschunginstitut Senckenberg 147, 215–223.

Bartiromo, A., Guignard, G., Barone-Lumaga, M.R., Barattolo, F., Chiodini, G., Avino, R., Guerriero, G., Barale, G., 2012. Influence of volcanic gases on the epidermis of *Pinus halepensis* Mill. In Campi Flegrei, Southern Italy: a possible tool detecting volcanism in present and past floras. J. Volcanol. Geotherm. Res. 233–234, 1–17.

Bartiromo, A., Guignard, G., Barone-Lumaga, M.R., Barattolo, F., Chiodini, G., Avino, R., Guerriero, G., Barale, G., 2013. The cuticle micromorphology of in situ *Erica arborea*

L. exposed to long-term volcanic gases in Phlegrean Fields, Campania, Italy. Environ. Exp. Bot. 87, 197–206.
Benikhlef, L., L'Haridon, F., Abou-Mansour, E., Serrano, M., Binda, M., Costa, A., Lehmann, S., Métraux, J.P., 2013. Perception of soft mechanical stress in *Arabidopsis* leaves activates disease resistance. BMC Plant Biol. 13, 133.
Braun, C.F.W., 1843. Beiträge zur Urgeshichte der Pflanzen. In: Muenster, G.G. (Ed.), Beiträge zur Petrefactenkunde 6. F. C. Birmer, Bayreuth, pp. 1–25.
Carrizo, M.A., Del Fueyo, G.M., Medina, F., 2014. Foliar cuticle of *Ruflorinia orlandoi* nov. sp. (Pteridospermophyta) from the Lower Cretaceous of Patagonia. Geobios 47, 87–99.
Cui, J.Z., 1995. Studies on the fusainized-wood fossils of Podocarpaceae from Huolinhe Coalfield, Inner Mongolia, China. Acta Bot. Sin. 37, 636–640 (in Chinese with English abstract).
D'Angelo, J.A., Zodrow, E.L., 2011. Chemometric study of functional groups in different layers of *Trigonocarpus grandis* ovules (Pennsylvanian seed fern, Canada). Org. Geochem. 42, 1039–1054.
D'Angelo, J.A., Zodrow, E.L., Camargo, A., 2010. Chemometric study of functional groups in Pennsylvanian gymnosperm plant organs (Sydney Coalfield, Canada): implications for chemotaxonomy and assessment of kerogen formation. Org. Geochem. (12), 1312–1325.
D'Angelo, J.A., Escudero, L.B., Volkheimer, W., Zodrow, E.L., 2011. Chemometric analysis of functional groups in fossil remains of the *Dicroidium* flora (Cacheuta, Mendoza, Argentina): implications for kerogen formation. Int. J. Coal Geol. (2), 97–111.
D'Angelo, J.A., Zodrow, E.L., Mastalerz, M., 2012. Compression map, functional groups and fossilization: a chemometric approach (Pennsylvanian neuropteroid foliage, Canada). Int. J. Coal Geol. 90, 149–155.
Del Fueyo, G., Villar de Seoane, L., Archangelsky, S., Guignard, G., 2006. Estudios cuticulares de *Ginkgoites* Seward del Cretácico Inferior de Patagonia. Revista del Museo Argentino de Ciencias Naturales NS. 8, 143–149.
Del Fueyo, G., Guignard, G., Villar De Seoane, L., Archangelsky, S., 2013. Leaf cuticle anatomy and the ultrastructure of *Ginkgoites ticoensis* Archang. from the Aptian of Patagonia. Int. J. Plant Sci. 174, 406–424.
Deng, S.H., 1995. Early Cretaceous Flora of Huolinhe Basin, Inner Mongolia, Northeast China. Geological Publishing House, Beijing (in Chinese with English summary.
Dominguez, E., Heredia-Guerrero, J.A., Heredia, A., 2011. The biophysical design of plant cuticles: an overview. New Phytol. 189, 938–949.
Elliott-Kingston, C., Haworth, M., McElwain, J.C., 2014. Damage structures in leaf epidermis and cuticle as an indicator of elevated atmospheric sulphur dioxide in early Mesozoic floras. Rev. Palaeobot. Palynol. 208, 25–42.
Elshatshat, S., Schreiber, L., Schönherr, J., 2007. Some cesium and potassium salts increase the water permeability of astomatous isolated plant cuticles. J. Plant Nutr. Soil Sci. 170, 59–64.
Fernández, V., Brown, P.H., 2013. From plant surface to plant metabolism: the uncertain fate of foliar-applied nutrients. Front. Plant Sci. 1–5.
Fernández, V., Eichert, T., 2009. Uptake of hydrophilic solutes through plant leaves: current state of knowledge and perspectives of foliar fertilization. Crit. Rev. Plant Sci. 28, 36–68.
Fernández, V., Guzmán-Delgado, P., Graça, J., Santos, S., Gil, L., 2016. Cuticle structure in relation to chemical composition: re-assessing the prevailing model. Front. Plant Sci. 7, 1–14.
Fischer, D.A., Bayer, D.E., 1972. Thin section of plant cuticles, demonstrating channels and wax platelets. Can. J. Bot. 50, 1509–1511.
Grammatikopoulos, G., Kyparissis, A., Drilias, P., Petropoulos, Y., Manetas, Y., 1998. Effects of UV-B radiation on cuticle thickness and nutritional value of leaves in two mediterranean evergreen sclerophylls. J. Plant Physiol. 153, 506–512.
Guan, Z.J., Zhang, S.B., Guan, K.Y., Li, S.Y., Hu, H., 2011. Leaf anatomical structures of *Paphiopedilum* and *Cypripedium* and their adaptive significance. J. Plant Res. 124, 289–298.
Guignard, G., Zhou, Z.H., 2005. Comparative studies of leaf cuticle ultrastructure between living and the oldest known fossil ginkgos in China. Int. J. Plant Sci. 166, 145–156.
Guignard, G., Thevenard, F., van Konijnenburg-van Cittert, J.H.A., 1998. Cuticle ultrastructure of the cheirolepidiaceous conifer *Hirmeriella muensteri* (Schenk) Jung. Rev. Palaeobot. Palynol. 104, 115–141.
Guignard, G., Boka, K., Barbacka, M., 2001. Sun and shade leaves? Cuticle ultrastructure of Jurassic *Komlopteris nordenskioeldii* (Nathorst) Barbacka. Rev. Palaeobot. Palynol. 114, 191–208.
Guignard, G., Popa, M., Barale, G., 2004. Ultrastructure of Early Jurassic fossil plant cuticles: *Pachypteris gradinarui* Popa. Tissue Cell 36, 263–273.
Guignard, G., Del Fueyo, G.M., Villar de Seoane, L., Carrizo, M.A., Lafuente Díaz, M.A., 2016. Insights into the leaf cuticle fine structure of *Ginkgoites skottsbergii* Lund. from the Albian of Patagonia and its relationship within Ginkgoaceae. Rev. Palaeobot. Palynol. 232, 22–39.
Guignard, G., Yang, X.J., Wang, Y.D., 2017. Cuticle ultrastructure of *Pseudofrenelopsis gansuensis*: further taxonomical implications for Cheirolepidiaceae. Cretac. Res. 71, 24–39.
Guzmán-Delgado, P., Graçab, J., Cabralb, V., Gil, L., Fernández, V., 2016. The presence of cutan limits the interpretation of cuticular chemistry and structure: *Ficus elastica* leaf as an example. Physiol. Plant. 157, 205–220.
Harris, T.M., Millington, W., Miller, J., 1974. The Yorkshire Jurassic flora IV. British Museum (Natural History), London.
He, D.C., 1995. The Coal-Forming Plants of Late Mesozoic in Da Hinggan Mountains. China Coal Industry Publishing House, Beijing (in Chinese and English).
Jeffree, C.E., 2006. The fine structure of the plant cuticle. In: Riederer, M., Müller, C. (Eds.), Biology of the Plant Cuticle. Blackwell, UK, USA, Australia, p. 461.
Kirchner, M., 1992. Untersuchungen an einigen Gymnospermen der fränkischen Rhät-Lias-Grenzschichten. Palaeontogr. B 224, 17–61.
Lugardon, B., 1971. Contribution à la connaissance de la morphogénèse et de la structure des parois sporales chez les Filicinées isosporées. Unpublished Thesis. Toulouse University, France (in French).
Mairot, C., Guignard, G., Yang, X.J., Zhou, Z.Y., 2014. Cuticle micro-and ultrastructure of *Suturovagina* Chow et Tsao (Cheirolepidiaceae): taxonomic and palaeoecological implications. Rev. Palaeobot. Palynol. 205, 9–21.
Niklas, K.J., 1983. Organelle preservation and protoplast partitioning in fossil angiosperm leaf tissues. Am. J. Bot. 70, 543–548.
Niklas, K.J., Brown, R.M., 1981. Ultrastructural and paleobiochemical correlations amongfossil leaf tissues from the St. Maries River (Clarkia) Area, Northern Idaho, USA. Am. J. Bot. 68, 332–341.
Niklas, K.J., Brown, R.M., Santos, R., Vian, B., 1978. Ultrastructure and cytochemistry of Miocene angiosperm leaf tissues. Proc. Natl Acad. Sci. USA 75, 3263–3267.
Niklas, K., Brown, R.M., Santos, R., 1985. Ultrastructural states of preservation in *Clarkia* angiosperm leaf tissues: implications on modes of fossilization. In: Smiley, C.J. (Ed.), Late Cenozoic History of the Pacific Northwest. American Association for Advancement of Science, Pacific Division, San Francisco, pp. 143–159.
Nosova, N., Yakovleva, O., Ivanova, A., Kiritchkova, A., 2016. First data on the ultrastructure of the leaf cuticle of a Mesozoic conifer, *Mirovia Reymanówna*. Rev. Palaeobot. Palynol. 233, 115–124.
Nosova, N., Yakovleva, O., Kotina, E., 2019. First data on the leaf cuticle ultrastructure of of the Mesozoic genus *Pseudotorellia* Florin. Rev. Palaeobot. Palynol. (this issue).
Passalia, M.G., Del Fueyo, G., Archangelsky, S., 2010. An Early Cretaceous zamiaceous cycad of South West Gondwana: *Restrepophyllum* nov.gen. from Patagonia, Argentina. Rev. Palaeobot. Palynol. 161, 137–150.
Rashidi, F., Jalili, A., Kafaki, S.B., Sagheb-Talebi, K., Hodgson, J., 2012. Anatomical responses of leaves of Black Locust (*Robinia pseudoacacia* L.) to urban pollutant gases and climatic factors. Trees 26, 363–375.
Santrucek, J., Simanova, E., Karbulkova, J., Simkova, M., Schreiber, L., 2004. A new technique for measurement of water permeability of stomatous cuticular membranes isolated from *Hedera helix* leaves. J. Exp. Bot. (401), 1411–1422.
Schoenhut, K., Vann, D.R., Le Page, B.A., 2004. Cytological and ultrastructural preservation in Eocene *Metasequoia* leaves from the Canadian High Arctic. Am. J. Bot. 91, 816–824.
Schönherr, J., 2002. Foliar nutrition using inorganic salts: laws of cuticular penetration. Proceedings of the International Symposium on Foliar Nutrition of perennial Fruit Plants. Acta Hortic. 594, 77–84.
Schönherr, J., Luber, M., 2001. Cuticular penetration of potassium salts: effects of humidity, anions, and temperature. Plant Soil 236, 117–122.
Schreuder, M.D.J., Brewer, C.A., 2001. Persistent effects of short-term, high exposure to chlorine gas on physiology and growth of *Pinus ponderosa* and *Pseudotsuga menziesii*. Ann. Bot. 88, 197–206.
Shen, H.X., Du, K.H., Wang, X., 2016. Plant cytoplasm preservation in a baked root of *Abies*. Palaeoworld 25, 287–291.
Simioni, P.F., Eisenlohr, P.V., Gomes-Pessoa, M.J., Vieira da Silva, I., 2017. Elucidating adaptive strategies from leaf anatomy: do Amazonian savannas present xeromorphic characteristics? Flora 226, 38–46.
Somapala, K., Weerahewa, D., Thrikawala, S., 2016. Silicon rich rice hull amended soil enhances anthracnose resistance in tomato. Pro. Food Sci. 6, 190–193.
Steinthorsdottir, M., Elliott-Kingston, C., Bacon, K.L., 2018. Cuticle surfaces of fossil plants as a potential proxy for volcanic SO2 emissions: observations from the Triassic–Jurassic transition of East Greenland. Palaeobiol. Palaeoenviron. 98, 49–69.
Stoyko, S.S., Rudyk, B.W., Mar, A., Zodrow, E.L., D'Angelo, J.A., 2013. Powder X-ray diffraction and X-ray photoelectron spectroscopy of cutin from a 300 Ma tree fern (*Alethopteris pseudograndinioides*, Canada). Int. J. Coal Geol. 106, 35–38.
Sun, G., 1987. Cuticles of *Phoenicopsis* from NE China with discussion on its taxonomy. Acta Palaeontol. Sin. 26, 662–688 in Chinese with English summary.
Sun, G., 1993. *Ginkgo coriacea* Florin from lower cretaceous of Huolinhe, northeastern Nei Mongol, China. Palaeontogr. B 230, 159–168.
Sun, G., Cao, Z.-Y., Li, H.-M., Wang, X.-F., 1995. Cretaceous floras. Editor-in-Chief. In: Li, X.X. (Ed.), Fossil Floras of China Through the Geological Ages. Guangdong Science and Technology Press, Guangzhou, pp. 411–454.
Sun, G., Lydon, S.J., Watson, J., 2003. *Sphenobaiera ikorfatensis* (Seward) Florin from the Lower Cretaceous of Huolinhe, eastern Inner Mongolia, China. Palaeontology 46, 423–430.
Thévenard, F., Barale, G., Guignard, G., Daviero-Gomez, V., Gomez, B., Philippe, M., Labert, N., 2005. Reappraisal of the ill-defined Liassic pteridosperm *Dichopteris* using an ultrastructural approach. Bot. J. Linn. Soc. Lond. 149, 313–332.
Tyree, M.T., Tabor, C.A., Wescott, C.R., 1990. Movement of cations through cuticles of *Citrus aurantium* and *Acer saccharum*. Diffusion potentials in mixed salt solutions. Plant Physiol. 94, 120–126.
Vachrameev, V.A., 1991. Jurassic and Cretaceous Floras and Climates of the Earth. Cambridge University Press, Cambridge.
Villar de Seoane, L., 1997. Comparative study between *Gingkoites tigrensis* Archangelsky and *Gingko biloba* leaves. Palaeobotanist 46, 1–12.
Villar De Seoane, L., 1998. Comparative study of extant and fossil conifer leaves from the Baqueró Formation (Lower Cretaceous), Santa Cruz Province, Argentina. Rev. Palaeobot. Palynol. 99, 247–263.
Villar de Seoane, L., 1999. *Otozamites ornatus* sp. nov., a new bennettitalean leaf species from Patagonia, Argentina. Cretac. Res. 20, 499–506.
Villar de Seoane, L., 2001. Cuticular study of Bennettitales from the Springhill Formation, Lower Cretaceous of Patagonia, Argentina. Cretac. Res. 22, 461–479.
Villar de Seoane, L., 2003. Cuticle ultrastructure of the Bennettitales from the Anfiteatro de Ticó Formation (Early Aptian), Santa Cruz Province, Argentina. Rev. Palaeobot. Palynol. 127, 59–76.
Villar de Seoane, L., 2005. New cycadalean leaves from the Anfiteatro de Ticó Formation, Early Aptian, Patagonia, Argentina. Cretac. Res. 26, 540–550.

Wang, Y.D., 2002. Fern ecological implications from the Lower Jurassic in Western Hubei, China. Rev. Palaeobot. Palynol. 119, 125–141.
Wang, Y.D., Mei, S.W., 1999. Fertile organs and *in situ* spores of a matoniaceous fern from the Lower Jurassic of West Hubei. Chin. Sci. Bull. 44, 1333–1337.
Wang, Y.D., Guignard, G., Thévenard, F., Dilcher, D., Barale, G., Mosbrügger, V., Yang, X.J., Mei, S.W., 2005. Cuticular Anatomy of *Sphenobaiera huangii* (Ginkgoales) from the Lower Jurassic of Hubei, China. Am. J. Bot. 92, 709–721.
Wattendorff, J., 1992. Cryoultrasections of *Agave americana* cuticles extracted for cuticular lipids: time-dependant penetration of KMnO4 and changes of the lamellar structure. Ann. Sixth Cell Wall Meet. Nijmegen Netherlands 1–68.
Wattendorff, J., Holloway, P.J., 1980. Studies on the ultrastructure and histochemistry of plant cuticles: the cuticular membrane of *Agave americana* L. *in situ*. Ann. Bot. 46, 13–28.
Wattendorff, J., Holloway, P.J., 1982. Studies on the ultrastructure and histochemistry of plant cuticles: isolated cuticular membrane preparations of *Agave americana* L. and the effects of various extraction procedures. Ann. Bot. 49, 769–804.
Wu, X.W., Yang, X.J., Zhou, Z.Y., 2006. Ginkgoalean ovulate organs and seeds associated with *Baiera furcata*-type leaves from the Middle Jurassic of Qinghai Province, China. Rev. Palaeobot. Palynol. 138, 209–225.
Yang, X.J., Guignard, G., Thévenard, F., Wang, Y.D., Barale, G., 2009. Leaf cuticle ultrastructure of *Pseudofrenelopsis dalatzensis* (Chow et Tsao) Cao ex Zhou (Cheirolepidiaceae) from the Lower Cretaceous Dalazi Formation of Jilin, China. Rev. Palaeobot. Palynol. 153, 8–18.
Yang, X.-J., Wang, Y.-D., Zhang, W., 2013. Occurrences of Early Cretaceous fossil woods in China: implications for paleoclimates. Palaeogeogr. Palaeoclimatol. Palaeoecol. 385, 213–220.
Yang, X.J., Guignard, G., Zhou, Z.-Y., Xu, Q., 2018. *Suturovagina intermedia* (Cheirolepidiaceae) from the upper Lower Cretaceous Dalazi Formation of Wangqing, Northeast China: cuticle ultrastructure and palaeoenvironmental insights. Cretac. Res. 91, 80–99.
Zhou, Z.Y., 2009. An overview of fossil Ginkgoales. Palaeoworld 18, 1–22.
Zhou, Z.Y., Guignard, G., 1998. Leaf cuticle ultrastructure of two czekanowskialeans from the Middle Jurassic Yima Formation of Henan, China. Rev. Palaeobot. Palynol. 102, 179–187.
Zhou, Z.Y., Wu, X.W., 2006. The rise of ginkgoalean plants in the early Mesozoic: a data analysis. Geol. J. 41, 363–375.
Zhou, Z.Y., Zhang, B.L., 1992. *Baiera hallei* Sze and associated ovule-bearing organs from the Middle Jurassic of Henan, China. Palaeontogr. B 224, 151–169.
Zhou, Z.Y., Thévenard, F., Barale, G., Guignard, G., 2000. A new xeromorphic conifer from the Cretaceous of East China. Palaeontology 43, 561–572.
Zhou, Z.Y., Yang, X.J., Wu, X.W., 2019. Ginkgophytes, Palaeoboanica Sinica. Science Press, Beijin in press.
Zodrow, E.L., Mastalerz, M., 2007. Functional groups in a single pteridosperm species: variability and circumscription (Pennsylvanian, Nova Scotia, Canada). Int. J. Coal Geol. 70, 313–324.
Zodrow, E.L., D'Angelo, J.A., Mastalerz, M., Cleal, C.J., Keefe, D., 2010. Phytochemistry of the fossilized-cuticle frond *Macroneuropteris macrophylla* (Pennsylvanian seed fern, Canada). Int. J. Coal Geol. 84, 71–82.
Zodrow, E.L., D'Angelo, J.A., Taylor, W.A., Catelani, T., Heredia-Guerrero, J.A., Mastalerz, M., 2016. Secretory organs: Implications for lipoid taxonomy and kerogen formation (seed ferns, Pennsylvanian, Canada). Int. J. Coal Geol. 167, 184–200.